THE EFFECT OF MICROSTRUCTURE ON THE FATIGUE CRACK GROWTH RESISTANCE OF NICKEL BASE SUPERALLOYS

Randy Bowman and Stephen D. Antolovich

School of Materials Engineering
Mechanical Properties Research Lab
Georgia Institute of Technology
Atlanta, Georgia 30332-0245

Abstract

The micro-mechanisms responsible for influencing fatigue crack propagation (FCP) in nickel base superalloys were investigated. Four experimental alloys were developed such that the lattice mismatch (δ), antiphase boundary energy (APBE), and volume fraction (V_f) of γ' precipitates were systematically varied. Heat treatments were also employed to obtain various grain and γ' sizes.

Constant amplitude cyclic loading revealed distinct differences in the FCP response of the four alloys. Precise load-displacement determinations indicated that crack closure was not responsible for these differences. The strength-normalized results indicate that those microstructures which can best accommodate damage are most resistant to crack growth. This is consistent with the accumulated damage model of FCP. Alloys with low V_f, low δ, and low APBE exhibited FCP rates that were approximately 50 times lower than for other treatments. FCP rates were dramatically reduced for those compositions and heat treatments that promoted planar, reversible slip. The effects of individual microstructural features on FCP rates were also determined.

Superalloys 1988
Edited by S. Reichman, D.N. Duhl,
G. Maurer, S. Antolovich and C. Lund
The Metallurgical Society, 1988

Introduction

The use of superalloys as jet engine components covers a period of nearly 40 years. The early applications were as blade materials and constituted approximately 10% of the weight of the engine. Current applications now include blades, high temperature turbine and compressor discs, nozzle guide vanes, and combustion chambers [1].

Fatigue crack propagation (FCP) was chosen as the basis for this study since the introduction of the retirement-for-cause (RFC) philosophy has made FCP a design-critical property for turbine disks. Because disks constitute up to 30% of the total engine weight, improvements in FCP could result in significant savings of expensive strategic materials while increasing the margin of safety.

Not only is quantification of fatigue damage an elusive goal but defining "damage" is open to debate. The most appealing way to make progress in defining and improving FCP resistance is to work on microstructurally simple systems in which important parameters can be varied systematically. In this way the importance of slip mode, precipitate coherency, crystal structure, etc., can be established as related to FCP. The body of this paper describes the results of such a study.

Background

Deformation of Ni Base Superalloys

Cutting of the γ' by dislocations produces an antiphase boundary (APB) resulting in an overall increase of energy. Paired dislocations are very common during particle cutting where the first dislocation creates the APB and passage of the second restores the stacking sequence thus eliminating the fault. Alloys with combinations of large γ' particles, low volume fractions and high lattice mismatch promote deformation by Orowan looping. In order for shearing to occur the stress necessary for particle cutting must be less than the Orowan looping stress. Both the shearing and looping stresses are a function of the γ' properties and particle size thus allowing the deformation process to be controlled through manipulation of microstructure and chemistry. Particle shearing causes dislocation pairing, makes cross-slip difficult and thus promotes inhomogeneous planar deformation. Cutting of fine precipitates leads to softening in the active slip bands.

The parameters described above can be controlled by composition and heat treatment modifications as described elsewhere [2].

Fatigue Crack Propagation

Antolovich and co-authors [3,4] proposed modifications to an earlier theory [5] in which FCP was viewed as an LCF process occurring out to a distance ρ ahead of the main crack tip. In this model, FCP is caused by damage accumulation in small elements that undergo reversed yielding. The crack then advances by some distance when sufficient damage has

accumulated in this "process zone". It was found that longer FCP lives were associated with larger process zones. The larger the process zone the smaller the average strain and the greater the number of cycles required to accumulate a critical amount of damage and advance the crack. Large grain sizes increase the process zone and should reduce FCP rates. This effect can be magnified by promoting slip reversibility (e.g. low mismatch and low APBE).

Alternatively, other authors [e.g. 6-8] attribute the lower FCP rates in coarse grain materials to increased crack closure. Closure reduces the stress intensity due to crack tip shielding of the remotely applied load. These studies found that the improvements in FCP resistance with the larger grains did not exist at high R -ratios where closure does not occur. Coarse and fine grained materials had nearly the same growth rates for R = 0.8. The explanation was that the larger grain sizes increased the fracture surface roughness resulting in more roughness induced closure. Also, the larger grains and correspondingly rougher surfaces had longer effective crack paths. Both of these effects contribute to a reduction in the FCP rates.

Research Program

Alloy Compositions

The controlled microstructural variables included APBE (Γ), mismatch (δ), and volume fraction of γ' (V_f). In addition, grain size (not reported in detail here) and γ' size were controlled by heat-treatments. These variables were chosen since they have all been shown to influence the deformation mode and, presumably, damage accumulation. The compositions and relative target levels for the control variables are shown in Table I.

Antiphase Boundary Energy, Mismatch and Volume Fraction

Control of antiphase boundary energy (APBE) was achieved through manipulation of the Ti/Al ratio. APBE was determined by measuring the spacing of dislocation pairs which are separated by the faulted region.

Table I. Alloy Compositions in Weight Percent and Associated Properties

Alloy	Ni	Al	Ti	Mo	Cr	B	Γ	δ	V_f
1	Bal	2.35	<.01	<.01	13.83	.0037	low	low	low
2	Bal	4.92	<.01	<.01	14.18	.0042	low	low	high
3	Bal	2.96	2.58	<.01	9.39	.0037	low	high	low
4	Bal	1.24	3.71	9.91	13.21	.0060	high	low	high

The effect of mismatch was investigated by producing alloys with low APBE and low V_f while varying the Ti content. It was calculated from the lattice parameter of the matrix and precipitate as determined using x-ray diffractometry.

The V_f of γ' is directly related to the amount of Al + Ti available for precipitation and was measured by phase extraction. Details of all measurement techniques as well as complete rationales are given elsewhere [9].

Mechanical Testing

Tensile specimens were tested to failure under strain control at a rate of 50%/min at room temperature to provide information on yield stress and Young's modulus. In addition, TEM examination of the tested specimens provided information concerning the deformation mode for each composition.

Two types of LCF tests were conducted. The first was a total strain controlled (0-tension-0) test to failure while the other was a interrupted constant plastic strain controlled test. All specimens were electrolytically polished prior to testing [9].

FCP tests were performed at room temperature using a closed loop servo-hydraulic test machine. Testing started in the near-threshold region and covered approximately three decades in growth rate. Crack lengths were monitored with a d-c potential drop system. In addition, crack closure was measured by compliance (load/displacement) techniques. Testing was performed at an R-ratio of 0.1 and 0.8 to examine the effect of closure. Full experimental details are given elsewhere [9].

Results and Discussion

This section describes the results obtained on the small grained alloys designated as indicated in Table I. For ease of presentation, the alloys were numbered according to their composition and gamma prime size. Therefore alloy number one with small γ' size is referred to as 1S while the large γ' material is 1L, etc. A summary of the alloys' properties is presented in Table II.

Initial Microstructures

The alloys were formed into "pancakes" by Wyman-Gordon prior to specimen fabrication. The grain size was very uniform across the entire cross section with an average grain size number of 8 for the small grained material. This uniformity of grain size in the pancake is essential to facilitate comparisons. Metallography of the ingots showed them to be free from any defects such as inclusions , porosity, etc. The γ' was unresolvable by optical microscopy for the S series of alloys whereas in the L series the γ' was clearly visible. There was some preference for γ' formation along the grain boundaries in the L series but the distribution was relatively homogeneous throughout the matrix.

To better characterize the γ' phase, transmission electron microscope (TEM) studies were undertaken on the initial structures. The γ' size in the L series alloys was seen to be approximately 0.6 μm whereas the small γ' material had precipitate sizes of around 0.08 μm. Higher magnification dark field images revealed the presence of hyperfine γ' particles in

all alloys with an average size of 0.008 μm. The γ' morphology ranged from spherical in alloy 1, the low mismatch alloy, to a blocky form in the larger mismatch system of alloy 4. Such morphologies are entirely consistent with basic physical metallurgy principles. In the untested condition, the dislocation density is seen to be very low. Only isolated dislocations, which were probably generated during forging and machining, were present.

TABLE II. Measured Microstructural Properties

Alloy	grain size (μm)	γ' size (μm)	Γ (ergs/cm^2)	δ (%)	V_f (%)	σ_{ys} (ksi)	ε_f (%)
1S	52	0.08	56	.09	21	30.31	54.9
1L	55	0.50	80	.07	21	32.60	49.6
2S	51	0.09	124	.07	27	88.68	36.6
2L	52	0.62	198	.04	25	100.00	31.2
3S	36	0.07	96	.21	21	94.30	32.8
3L	42	0.54	120	.18	18	108.40	31.6
4S	23	0.07	420	.18	25	94.30	48.4
4L	34	0.68	403	.14	22	93.20	42.3

Tensile Properties

Monotonic tensile properties for all alloys are summarized in Table II. Yield stress values for each alloy are qualitatively consistent with those predicted from deformation models as discussed in detail elsewhere [9].

Fatigue Crack Propagation

In Fig. 1a, the FCP response of the small γ' alloys tested at an R-ratio of 0.1 at room temperature in air is presented. Correlation of FCP rates as a function of ΔK describes a material's response to cyclic loading. Crack extension at a given value of ΔK is a function of both the amount of damage imposed at the crack tip and the material's intrinsic ability to accommodate the damage. For a given stress level, an alloy with a low yield stress but high resistance to crack extension can exhibit the same FCP rate as an alloy with a high yield strength and low crack growth resistance. Most FCP models predict an inverse relationship between crack growth rate and yield strength. It is therefore useful to attempt to normalize the FCP results with respect to yield strength thereby eliminating the differences in strength, Fig. 1b.

Examination of the fracture surface, Fig. 2, shows that roughness of the fracture surface arises due to cracking along slip bands which formed during the test. Roughness measurements of the fracture surfaces as a function of ΔK are presented in Fig. 3. The roughness parameter, R_L, is a measure of the actual crack path divided by the projected crack path. Comparison of these results with Fig. 1 shows that the specimens with the roughest surfaces have the greatest

resistance to crack growth while the specimens with a relatively smooth fracture surface have the highest growth rate. Initially this seems to imply that FCP is controlled by a roughness induced closure effect whereby the specimen with the largest surface roughness will have the most roughness induced crack closure and thus the lowest crack growth rate. This interpretation is discussed below.

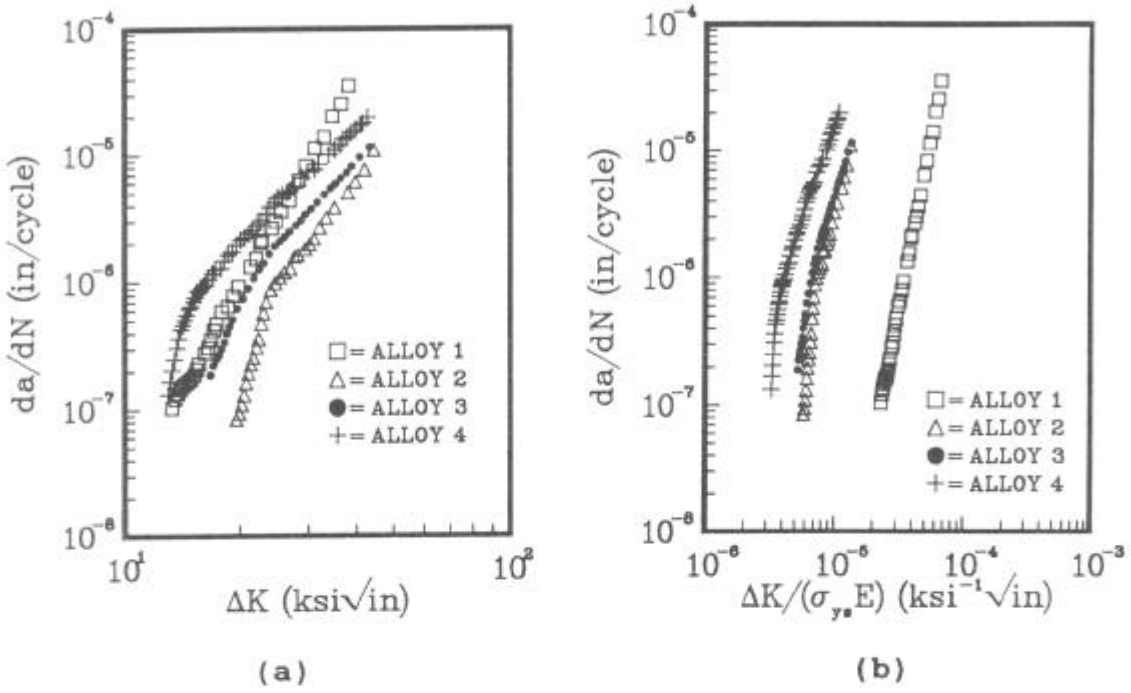

Figure 1 - FCP response of small γ' materials for R = 0.1. In (b) the data is normalized with respect to yield strength and elastic modulus.

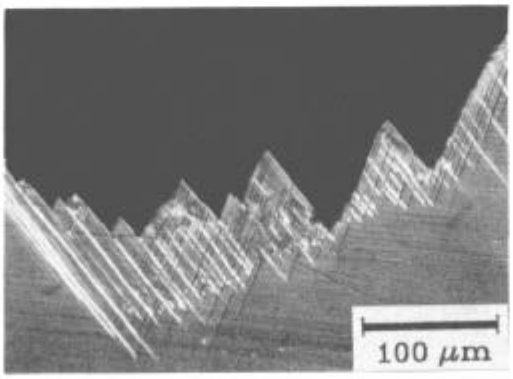

Figure 2 - Optical micrograph of alloy 4S fracture profile.

Closure

To investigate the importance of roughness, closure measurements were performed [9] at R=0.1 and at R=0.8, Fig. 4. Load-line/displacement measurements indicated a closure load of approximately $0.1P_{max}$ for all alloys at near threshold regions

which decreased to zero in the mid-Paris regime. Since the closure loads were similar and relatively low for all alloys, no significant difference in the growth rates was noted when plotted vs. ΔK_{eff} ($\Delta K_{eff} = \Delta K_{max} - \Delta K_{cl}$). The **apparent** correlation between surface roughness and FCP rates (i.e. large roughness associated with low growth rates) can not be explained on the basis of roughness induced closure, however appealing this explanation may be.

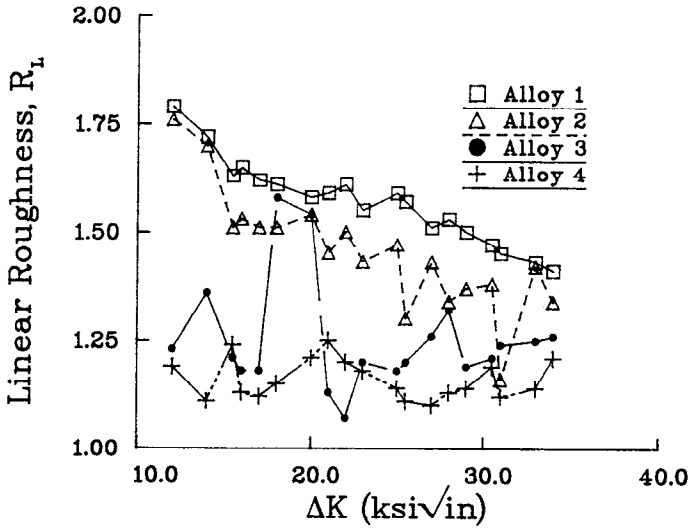

Figure 3 - Fracture surface roughness as a function of stress intensity level.

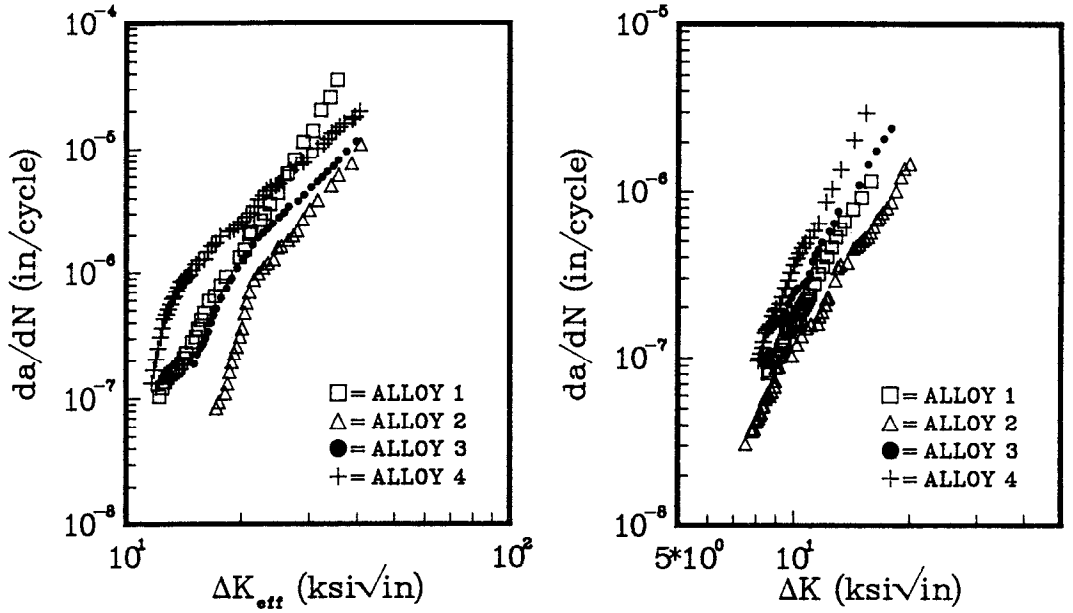

Figure 4 - FCP response of small γ' materials. a) results plotted versus ΔK_{eff} thus accounting for crack closure. b) material response at R = 0.8.

At R = 0.8 (no closure), the relative FCP rates were unchanged although the absolute values of da/dN at R = 0.8 were higher due the larger mean stress. It is clear that the observed differences in growth rates for these alloys are due to "intrinsic" differences in fundamental micromechanical processes and not to "extrinsic" effects such as closure as is

often cited for other systems. With all "extrinsic" factors eliminated, the dominant features controlling FCP can be identified.

Low Cycle Fatigue

Total strain controlled tests resulted in an initial hardening response (increasing load) for alloys 1-3 followed by gradual softening over the remaining life of the tests. This behavior suggests that particle shearing is the dominant deformation mechanism for these alloys. Conversely, alloy 4 hardened to a saturation level, indicative of deformation by Orowan looping. The lives for alloys 1-3 were all very similar at the same strain levels (around 7500 cycles) whereas the life of alloy 4 (low strength, high ductility) was nearly 4 times as long.

Deformation Structures

TEM examination of the interrupted, constant plastic strain controlled tests indicated that the ability of alloys 1 and 2 to accommodate strain without the subsequent development of damage was very good (low dislocation density) whereas alloy 4 had nearly 5 times the dislocation density for the same imposed plastic strain. Alloys 1 and 2 had similar dislocation densities, any differences being hidden in the inaccuracies of the dislocation density measurement technique. The ability of a particular alloy to accommodate damage (as measured by the dislocation density) is directly related to the alloy's ability to resist crack growth. Specifically, alloy 1 had the lowest crack growth rate when normalized with respect to strength and it also had the lowest dislocation density under constant plastic strain controlled conditions. In this case many cycles must be imposed at the crack tip to reach the critical damage level necessary to advance the crack. Alloy 4 has poor resistance to damage and requires few cycles to accumulate the required damage necessary for crack advance.

Alloys 1S,2S, and 3S deformed by shearing (i.e.dislocation pairing, planar slip) while 4S deformed by looping. Representative micrographs are shown in Fig. 5. For shearing to occur the stress must be less than the Orowan looping stress. For alloy 4S, the APBE is sufficiently high to prevent shearing.

Any proposed model must account for different deformation modes depending on the specific alloy system and test conditions. Those factors which control FCP when the precipitates are sheared may not operate when dislocation by-pass occurs complicating interpretation of microstructural influences on FCP.

FCP of Small γ' alloys

From the da/dN vs. ΔK plots (Fig. 1b), it is clear that alloy 1S (low Γ, low δ, low V_f) is most resistant to crack advance. When normalized as described above, the FCP rate of this alloy system is at least two orders of magnitude slower than the others. The low volume fraction of precipitates results in a larger mean free path between obstacles for the

mobile dislocations. The imposed plastic strain is therefore more easily accommodated resulting in less damage accumulation and thus greater resistance to crack advance. The efficiency of the γ' as obstacles to dislocation motion is reduced further in this alloy by the low values of APBE and δ. Conversely, alloy 2S has the same APBE and δ but a much higher V_f of γ'. This combination results in relatively higher crack growth rates. The ability of this material to accommodate strain at the crack tip is reduced by the small mean free path of the dislocations.

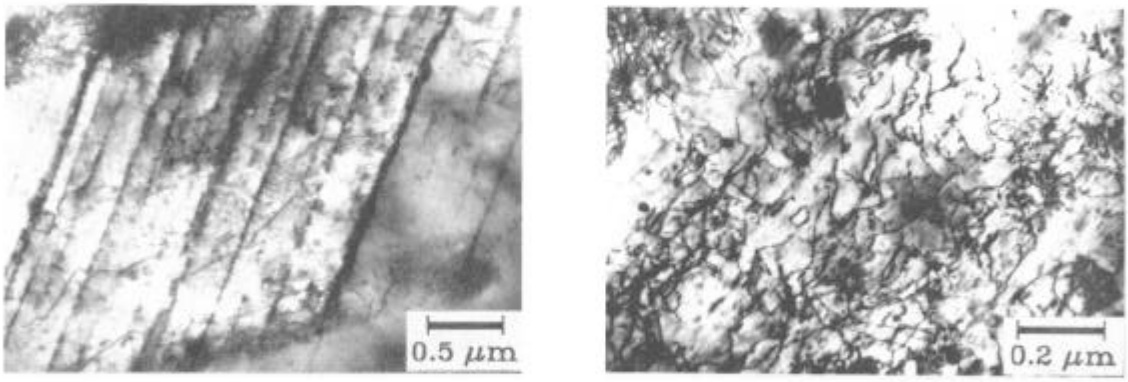

(a) (b)

Figure 5 - Representative deformation structures illustrating a) shearing, alloy 2S and b) looping, alloy 4S.

The decreased resistance to FCP due to higher APBE (alloy 4S) is due to the difference in deformation mode caused by the APBE. In the other S series alloys, which have various combinations of APBE and V_f, particle shearing occurs, Fig. 5, whereas for alloy 4S with a high APBE particle by-pass is the dominant deformation mode and no APBE is created (i.e. no energy increase). With particle looping, the contribution of δ toward inhibiting dislocation motion becomes more pronounced since in the looping regime the CRSS is directly related to mismatch.

For small γ' precipitates, alloys 2S and 3S had differences of 3-5 times in FCP rates due only to changes in mismatch and a slight difference in V_f. In fact, from the previous argument, increased V_f is seen to increase the FCP rate when normalized with respect to σ_{ys} and E due to a lowering of the mean free path. All other factors being constant, a lower volume fraction of precipitates should reduce the FCP rate. Therefore, the differences in the FCP response of alloys 2S and 3S is even greater if alloy 2S is shifted down in the FCP plot (or 3S is shifted up) to account for the difference in mean free path. The increase in FCP rate for the higher mismatch alloy is a result of the increased resistance to dislocation motion due to the enhanced strain field around the precipitate and/or a different deformation mode.

Summary

Constant amplitude FCP tests were performed on each of four alloy compositions with two different γ' sizes to investigate the effects of microstructure and composition.

The major findings and observations were:

1) Crack closure concepts do not explain differences in the FCP rates for both near threshold and Paris regime propagation in the model Ni base alloys studied here.

2) FCP rates are dramatically low for those compositions and treatments that promote planar, reversible slip.

3) In this study, alloys having high volume fraction, low APBE, and low mismatch exhibited FCP rates that were approximately fifty times lower than other alloys.

4) Internal resistance to damage ahead of a crack is achieved by low volume fraction of precipitates, low lattice mismatch, and low anti-phase boundary energy. FCP resistance is increased by a planar deformation mode. However, in a planar slip material, on a strength/modulus normalized basis, restricting dislocation motion decreases the alloy's ability to accommodate damage and increases the FCP rate.

5) At the same strength level, it has been demonstrated that the FCP rate can be reduced by at least a factor of 50.

6) The implications of this study are that FCP rates in alloys of practical interest can be significantly reduced by heat treatment and modest compositional changes.

Acknowledgements

The authors are grateful to the AFOSR for financial support of this research (Grant # AFOSR 84-0101, Dr. Alan H. Rosenstein Program Manager). They would also like to thank Dr. Hugh Gray of the NASA-Lewis Research Center for assistance in the alloy development phase of the work and Mr. W. Couts of Wyman-Gordon for his help in processing the alloys. One of us (RB) would also like to thank the Wyman-Gordon foundation for a Wyman-Gordon Fellowship.

References

1. J.E. King, Mat. Sci. and Tech., Vol. 3, 1987, pp. 750-764.
2. The Superalloys, C.T Sims and W.L. Hagel eds., John Wiley and Sons, Inc., New York, 1972.
3. G.R. Chanani, S.D. Antolovich, and W.W. Gerberich, Met. Trans., Vol. 3, 1972, pp. 2661-2672.
4. S.D. Antolovich, A. Saxena, and G.R. Chanani, Eng. Frac. Mech., Vol. 7, 1975, pp. 649-652.
5. F.A. McClintock, Fracture of Solids, D.C. Drucker and J. Gilman Eds., John Wiley and Sons, N.Y., 1963, pp. 65-102.
6. G.T. Gray III, J.C. Williams, and A.W. Thompson, Met. Trans., Vol 14, 1983, pp. 421-433.
7. Jian Ku Shang, J.-L. Tzou, and R.O. Ritchie, Met. Trans., Vol. 18, 1987, pp. 1613-1627.
8. R.D. Carter, E.W. Lee, E.A. Starke Jr., and C.J. Beevers, Met. Trans., Vol. 15, 1984, pp. 555-563.
9. R. Bowman, Ph.D. Dissertation, Georgia Institute of Technology, Atlanta, Georgia, 1988.